

Evolution of PVA gels prepared without crosslinking agents as a cell adhesive surface

Siddhi Gupta · Thomas J. Webster ·
Arvind Sinha

Received: 18 February 2011 / Accepted: 9 May 2011
© Springer Science+Business Media, LLC 2011

Abstract Physical parameters (such as crosslinking density, crystallinity and mechanical properties) have been found to largely affect cellular behavior on polymer scaffolds. This study demonstrated that transparent pure Poly (vinyl alcohol) hydrogels prepared via a freeze–thaw method can be made to support cell adhesion by controlling physical parameters such as concentration and the number of freeze–thaw cycles. For a given number of freeze–thaw cycles, (specifically 45), polymer concentration dependent structural and mechanical properties (such as tensile strength and stiffness) were correlated with cell adhesion. The maximum cell attachment occurred on the hydrogels with the greatest mechanical properties, crystallinity and crosslinking density. The hydrogel surfaces were more favorable to human dermal fibroblasts than human lens epithelial cells and retained their transparency as well as dimensional stability with only a small degree of swelling. Fibroblast laden hydrogels showed extensive alkaline phosphatase activity which confirmed their healthy proliferation and function. In this manner, this study suggests that transparent Poly (vinyl alcohol) hydrogels prepared by the freeze thaw method described here should be further studied for numerous tissue engineering applications.

1 Introduction

Hydrogels are increasingly becoming important materials amongst tissue engineers and material scientists for numerous biomedical applications [1–4]. The choice of polymer is crucial in this regard as it should possess a high degree of tailorability for the specific application of interest. Poly (vinyl alcohol) (PVA) is an excellent choice for tissue engineering applications as it can produce non-toxic and mechanically strong hydrogels by hydrogen bond induced crosslinking [5, 6]. PVA is a unique material as even in its atactic form and lack of stereo regularity, it is semi crystalline in nature. In aqueous solutions, entangled aggregates of hydrogen bonded PVA molecules are formed. Upon freezing the solutions, ice forms in the amorphous region and polymer crystallites grow until they meet the facets of other crystallites which assist in the formation of a porous network upon thawing. This is why these hydrogels possess better strength and stiffness than their chemically crosslinked counterparts as the mechanical load is distributed along the crystallites in the network [7–10]. PVA hydrogels prepared using freeze/thaw cycles are an obvious choice in this regard, as they exhibit a high degree of toughness, a rubbery elastic nature, are non-toxic, and can be readily accepted in the body [11, 12]. All this makes PVA preferable over other synthetic polymers from a biomimetic perspective, to be applied as matrices for tissue engineering applications and as a vehicle for the controlled release of drugs [13–16].

For tissue engineering applications, it is a general requirement that cells adhere to the surface of scaffolds and proliferate to eventually form a specific extracellular matrix (ECM). The suitability of PVA as a tissue engineering scaffold has been a debatable topic as many groups claim that the hydrophilic nature of PVA makes its surface subpar for cell attachment [17–19]. In the past, this

S. Gupta (✉) · A. Sinha
CSIR-National Metallurgical Laboratory, Council of Scientific
and Industrial Research, Jamshedpur, India
e-mail: siddhigupta@nmlindia.org

T. J. Webster
School of Engineering and Department of Orthopaedics,
Brown University, Rhode Island, USA
e-mail: Thomas_Webster@Brown.edu

problem has been tackled either by surface functionalization using ECM proteins (such as collagen, fibronectin, vitronectin, laminin, etc.) or synthetic ECM mimetic tripeptides (Arg-Gly-Asp/RGD). Other strategies include the incorporation of chitosan, blending with starch, gelatin, etc., interpenetration of acrylate polymers (specifically, polyhydroxyethylacrylate) into PVA, the creation of photolithographic patterns, etc. [20, 21]. All of these methods increase the complexity of the system and involve the use of chemicals to achieve suitable mechanical strength which ultimately produces toxic residues.

Thus, it is essential to design a scaffold with suitable properties without using toxic chemicals. Also, the process should be economically suitable in order to be commercially viable in the future. We have attempted to address this issue here by simply modifying the mechanical properties and wettability of PVA hydrogels maintaining their mechanical properties and transparency.

In the past, our group has already established the fabrication of freeze-thawed transparent PVA hydrogels synthesized without the aid of any crosslinkers and with a broad range of mechanical properties [22, 23]. It has also been observed by our research group that crystallinity and mechanical behavior of the transparent PVA hydrogels exhibit a systematic variation in properties as a function of both concentration as well as number of freeze-thaw cycles used. Further investigating the utility of these hydrogels as tissue engineering scaffolds, hydrogels with different polymer concentrations were fabricated here after 45 cycles of freeze-thawing and were tested *in vitro* with human dermal fibroblasts and human lens epithelial cells. The rationale behind using 45 cycles was the hypothesis that this would lead to the highest values in mechanical properties and crosslinking in the hydrogels as compared to those harvested after the initial 15 and 30 cycles. Due to their prolonged stability in aqueous medium and lowest swelling ratio, they were particularly chosen for cell culture experiments and so only those hydrogels are discussed here. The cellular adhesion and protein secretion results obtained during these experiments disproved previous reports which declared that the pure form of PVA is intrinsically non-adhesive to cells [17–19]. Thus, the present study demonstrates how one can tailor the composition, mechanical properties and surface energy of PVA to influence cell attachment.

2 Materials and methods

2.1 Hydrogel synthesis

For the preparation of hydrogels, PVA was purchased from Acros Organics, USA with a 95,000 da molecular weight and a 95% degree of hydrolysis. Sodium chloride,

potassium chloride, di sodium hydrogen phosphate and di hydrogen potassium phosphate (for preparation of phosphate buffer saline, PBS) were purchased from Sigma, USA. Malachite green phosphatase assay kits were purchased from Upstate Cell Signaling Solutions, USA.

PVA solutions (compositions: 10, 12, 14 and 16% wt/v) were prepared by dissolving appropriate amounts of PVA in distilled water with heating (at around 80°C) and constant stirring. After synthesis, PVA solutions were kept at room temperature so as to remove air bubbles. The solutions were poured into molds and subjected to repeated freeze-thawing cycles at temperatures of $0 \pm 2^\circ\text{C}$ (freezing) and $37 \pm 2^\circ\text{C}$ (thawing). After 15 cycles, a transparent hydrogel as shown in Fig. 1 was obtained. Freeze-thawing continued and specimens were cut from the bulk hydrogel sheet after 45 cycles and were used for characterization.

2.2 Structural characterization

2.2.1 X-ray diffraction

Wide angle X ray diffraction (XRD) profiles of PVA powder and uniform hydrogel films were collected at room temperature with a X-ray diffractometer (D8 Discover, Bruker) using $\text{CuK}\alpha$ radiation at 2θ degree ranges of 10° – 80° . The degree of crystallinity was computed manually by calculating the area under peaks from all XRD patterns of the hydrogels and was plotted as a function of PVA concentration.

2.2.2 Mechanical testing

The tensile tests of the hydrogels were carried out on a table top mechanical testing machine (Instron Electropuls E1000



Fig. 1 A transparent PVA hydrogel synthesized by freeze-thawing

K6301, UK) equipped with a dynamic capacity of 1000 N. Rectangular gel strips of approximately 16 mm length and 3.5 mm width were cut from the PVA hydrogel sheets with a thickness ranging between 0.19 and 0.22 mm. The ramp rate was maintained at 10 mm/min for all the hydrogel samples. During tests, the specimens were stretched to failure. From the original load-position data, the ultimate tensile strength and the Young's modulus were calculated. The values presented were averaged over 3 experiments and plotted as a function of PVA concentration.

2.2.3 Swelling tests

2.2.3.1 Swelling ratio and crosslinking density Equilibrium swelling experiments of all the hydrogels were carried out by immersing the hydrogels in distilled water at 37°C. The swollen samples were periodically taken out from water, excess water dried on a tissue paper, and weighed until no increase in weight was observed. The experiments were carried out three times for each sample, and the average values were computed manually using the following equations to obtain the swelling ratio and the crosslinking density, respectively:

Swelling ratio,

$$Q = W_f/W_i * 100$$

where, W_i is the initial weight of the hydrogel and W_f the final weight of the hydrogel.

Crosslinking density of the hydrogel was computed following the Flory Rehner equation which gave the value of M_c (average molecular weight between crosslinks). $1/M_c$ is taken as the crosslinking density. The equation is given below:

$$M_c = V_p + \chi(V_p)^2 + \ln(1 - V_p)/V_s d_r \left[(V_p)^{1/3} - V_p/2 \right]$$

where, χ is the polymer solvent interaction parameter (= 0.49), V_p the volume fraction of polymer in the swollen mass (calculated as $V_p = 1/(1+Q)$), V_s the molar volume of solvent, and d_r = density of polymer (1.2 g cm⁻³).

2.2.3.2 Optical contact angle and surface energy Optical contact angle measurements were carried out on an optical contact angle meter (Data Physics, OCAH 230, Germany). The surface energy and contact angles were recorded directly from the instrument software and plotted as a function of polymer concentration.

2.3 Cell culture experiments

2.3.1 Human dermal fibroblasts/human lens epithelial cells and optical microscopy

The human dermal fibroblasts and human lens epithelial cells were purchased from the American Type Culture

Collection (ATCC PCS-201-011 and ATCC CRL-11421 respectively, USA). The former were cultured in Dulbecco's modified eagle medium (DMEM, high glucose) supplemented with 10% fetal bovine serum (FBS) and a 1% Penicillin–Streptomycin (PS) solution. The DMEM was prepared by dissolving appropriate amounts of DMEM powder (Gibco) and Sodium bicarbonate, NaHCO₃ (Gibco) and filtered using membrane filters into pre-sterilized glassware. Cells lines were maintained at 37°C/5% CO₂ and the media was changed every 24 h. Fibroblasts divided rapidly with a doubling time of less than 48 h and attached on the culture flask within 4 h. For the human lens epithelial cells, the DMEM used was supplemented with 20% FBS and 1% PS. For these cells, the population doubling time was almost 7 days. Cell adhesion and multiplication were monitored at different cultivation times (4 h, 24 h and 3 days) by light microscopy using an inverted microscope.

2.3.2 Adhesion experiment and DAPI staining

The cells were harvested with a Trypsin-EDTA solution (with washing by Phosphate buffer saline to remove non adherent cells) and counted using a hemocytometer. The seeding density was 3500 cells/cm². Prior to the experiment, the hydrogels were kept in a 6 well culture plate and the surface was sterilized by spraying ethanol and exposure to UV light overnight (for 12 h). The wells with controls and hydrogels were filled with approximately 5 ml of DMEM. This was completed for 2 h before cell seeding so as to swell the hydrogels upto equilibrium. The glass coverslips were used as controls. The culture plates were kept in an incubator post cell seeding. After 4 h, the cells attached on PVA hydrogels were stained using the dye 4,6-diamidino-2-phenylindole or DAPI [24, 25]. For the staining protocol, first the cells were fixed using 10% formalin followed by a subsequent washing with PBS before adding 10 µl of DAPI (diluted with PBS at 1:30). After 20 min, the hydrogels were again washed with PBS (3 times). Finally, the samples were imaged using fluorescence microscopy (10×). For presentation, the attached cell nuclei were pseudo-colored in blue using Image Pro analyzer software. The cells were simply counted from the micrographs and an average cell count (from 5 pictures per sample) per substrate for each time point was plotted as a function of PVA concentration.

2.3.3 Alkaline phosphatase activity tests (malachite green phosphate assay)

Alkaline phosphatase (ALP) is an important enzyme synthesized by fibroblasts. To test this, the scaffolds were seeded with 1,000,000 cells/cm² and kept in an incubator for 7 days (medium changed every 24 h) following the procedure described above. After 7 days, the medium was

removed and cells were washed with Tris Buffer Saline (twice). After this, cell lysis was performed using repeated freeze–thaw cycles. The freeze–thaw cycles were conducted in a -80°C freezer for freezing and a 37°C incubator for thawing with 5 min of shaking (before placing the samples in the incubator) on a rotary shaker. After 5 cycles, the lysates were collected in separate tubes. For measuring the ALP activity, a specialized kit was used. Enzyme reactions were performed in a final volume of 25–50 μl (using the same volume as that used for the standard curve).

The assays were carried out in a 96 well microtiter plate. In brief, 5 μl BSA solution, an aliquot containing 0.1–0.5 μg of enzyme and 80 μl of pNPP Tyrosin assay buffer were mixed in a well. The blank was prepared the same way as the sample minus the enzyme. Pre-incubation was done for 15 min at 37°C to speed up the reaction. 120 μl of pNPP substrate solution was added to start the phosphatase reaction and was again incubated for 15 min at 37°C . The reaction was then stopped by adding 20 μl of stopping solution. The assay was read against the blank at 405–410 nm in a plate reader. The following equation was used to determine phosphatase activity:

$$\frac{(\text{Sample volume in liters}) \times A_{405}}{(\varepsilon) \times (\text{Pathlength of light in cm}^*) \times (\text{Assay time in minutes}) \times (\text{units or } \mu\text{g of enzyme})}$$

where (ε) is the extinction coefficient for pNPP at $A_{405} = 1.78 \times 10^4 \text{ M}^{-1} \text{ cm}^{-1}$, A_{405} is the phosphatase activity, and one unit of activity is equivalent to 1 mmol pNPP hydrolyzed per minute.

2.3.4 Statistical analysis

Experiments were conducted in triplicate and were averaged at which point a student *t*-test (paired) was performed to determined differences between means. Probability (*P*) values <0.5 , 0.05 and 0.005 were considered to indicate statistical differences. Error bars in the results of cell adhesion and ALP activity were expressed as mean \pm standard deviation ($n = 3$). Values were plotted as a function of hydrogel composition.

3 Results

3.1 Structural characterization

Figure 2a shows the powder X-ray diffraction (XRD) pattern of the parent material. The strong crystalline

reflections at $2\theta = 19.88^{\circ}$ and 20.18° ($d = 4.46$ and 4.39 , respectively) are characteristic of PVA [26]. The diffused peaks at higher angles confirm the semi-crystalline nature of the polymer. Figures 2b shows the XRD patterns of the hydrogel specimens after 45 cycles of freeze–thawing at PVA concentrations ranging from 10 to 16%. It can be visualized from the figure that the peaks are around $2\theta = 19.8^{\circ}$, i.e., the (101) diffraction of the PVA crystals are showing a clear difference in their intensities due to the changes in their degree of crystallinity. The (101) diffraction is due to the intermolecular interference between PVA chains in the direction of the intermolecular hydrogen bonding [27].

Figure 2c shows the variation of degree of crystallinity of the hydrogels as a function of PVA concentration. As the number of regularly arranged polymer chains is increasing with increasing polymer concentration in a given volume, the total volume fraction of crystalline regions also increases. This is accounted for in the increasing trend of the degree of crystallinity observed here.

3.1.1 Mechanical tests

The non-linear stress–strain curves for the as prepared PVA hydrogels obtained after 45 cycles of freeze–thawing were plotted from the data generated from the load–position diagram obtained by the instrument (Fig. 3a). Ultimate tensile strength could directly be recorded from the stress–strain curves; however, an estimate of the elastic modulus was made by drawing tangent lines within the elastic region of the curve. The variation in the Ultimate Tensile Strength (MPa) of the hydrogels as a function of PVA concentration is shown in Fig. 3b. The increasing trend confirms the fact that the degree of crystallinity and the mechanical strength of the hydrogels go hand in hand, i.e., the higher the crystallinity, the higher the ultimate strength of the polymeric network owing to the increased number of polymer crystallites and vice versa [10, 28, 29]. The point to be noted here is the significant contribution of the hydrogen bonded PVA crystallites in the network over which the mechanical load is distributed. This is the reason why physically crosslinked hydrogels exhibit much more strength and stability than the hydrogels prepared by other means [30, 31]. The highest value of the ultimate tensile

Fig. 2 **a** X ray diffraction pattern of pure PVA. **b** X ray diffraction pattern of the hydrogel samples showing an increase in the intensity of the peak corresponding to PVA(101). **c** Degree of crystallinity as calculated from the XRD curves of the hydrogel samples as a function of PVA concentration

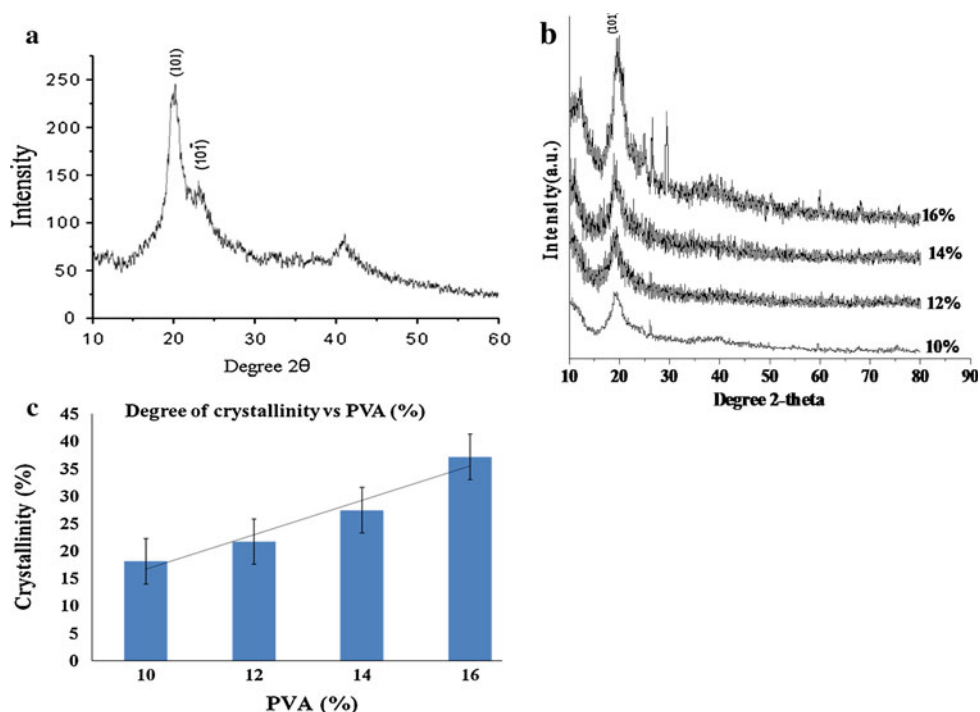
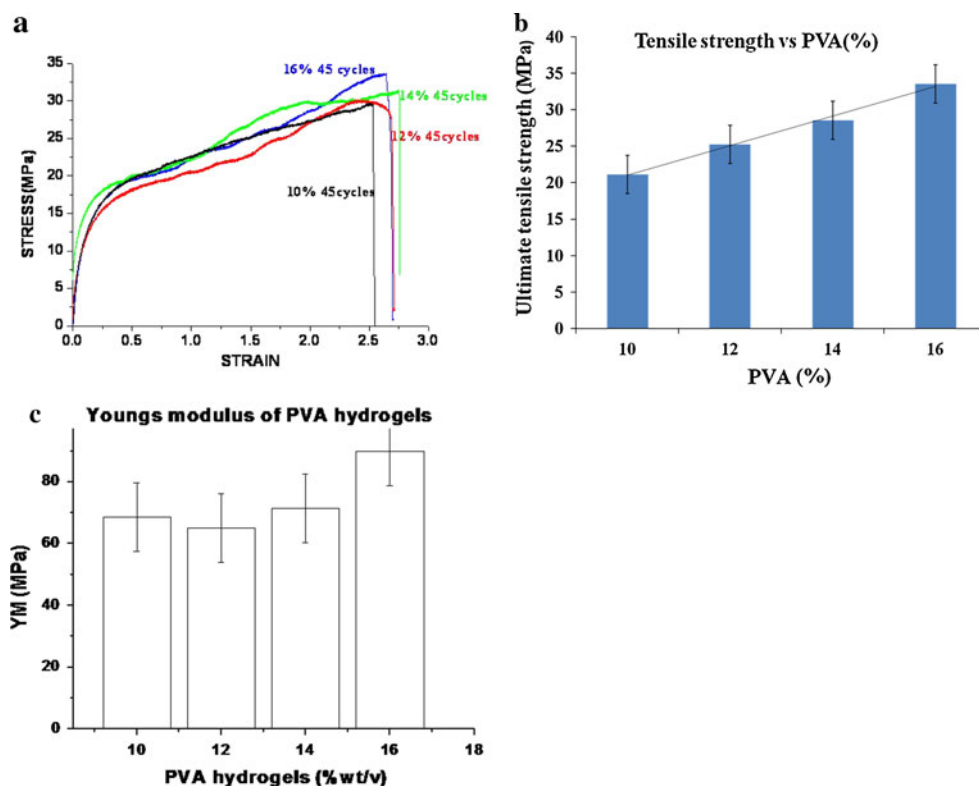


Fig. 3 **a** Stress–strain curves of the hydrogel samples as a function of PVA concentration. **b** Ultimate tensile strength (MPa) of PVA hydrogels as computed from the stress–strain curves. **c** Youngs modulus (MPa) of PVA hydrogels as computed by the stress strain curves



strength of 33.52 MPa was observed in the 16% PVA hydrogel which also had the highest degree of crystallinity. It is worth mentioning here that to date such a high strength could only be achieved either by the addition of a

crosslinking agent (either DMSO or HMDI) and at freezing temperatures -20°C or less [32]. Attainment of such a high strength coupled with transparency without invoking any chemical crosslinker at such low freezing temperatures

definitely provides an advantage of the presently fabricated material over other chemically crosslinked PVA scaffolds using such toxic entities.

Figure 3c presents the variation of the Young's modulus of the hydrogels as a function of PVA concentration. The highest value of modulus is around 90 MPa corresponding to the 16% PVA hydrogel. Hydrogel stiffness results from the available OH groups of PVA that participate in the hydrogen bonding. The intra- as well as inter-molecular hydrogen bonding between the pendant OH groups of PVA and water governs the crystallinity as well as the elasticity of the bulk PVA material and, thus, increases with increasing hydrogen bond interactions [33–35].

As per the present results, the stiffness range favorable for cells was found to be between 68 and 90 MPa for the transparent freeze-thawed PVA hydrogels. Material stiffness, as a property dependent upon polymer concentration, is a significant structural parameter that can be easily utilized and modified to achieve control over cell attachment [36, 37].

3.1.2 Swelling tests

The curve in Fig. 4a indicates a variation in the swelling ratio of the hydrogels as a function of PVA concentration and shows that the ratio of swelling decreases as the concentration increases. Swelling is directly dependent on the porosity of the hydrogel networks. The key factors which control pore volume fraction, pore sizes and their inter-connection are the composition of the network polymer chains and the crosslinking density. The increasing concentration of the polymer in a given volume happens to lead to an increase in the number of ordered polymer chains thereby decreasing the porosity in the network, which is most likely the reason for the decreased water holding capacity of the hydrogels [22].

As presented in the curves in Fig. 4b, the calculated crosslinking densities have been shown to increase as the PVA concentration increased. A higher degree of crosslinking results in smaller water uptake [38]. Therefore, this supports the crystallinity and tensile strength data given

above. Also, it was observed during the course of experiments that the presence of water (as well as culture medium during the in vitro tests) did not affect the transparency of the hydrogels. Swelling is an important property of the hydrogels and on the basis of our results, it is believed that it can be controlled to a certain extent by optimizing the polymer concentration and the number of freeze-thaw cycles.

3.1.3 Wettability

The wettability measurements plotted as a function of PVA concentration (Fig. 5a, b) demonstrate that contact angle and free surface energy are variable with the composition of the hydrogels. Specifically, the contact angle (or hydrophilicity) and surface energy shows a parabolic trend where up to 14% of hydrophilicity increased and dropped for the 16% hydrogel, which was the most crystalline hydrogel. Such a trend has been reported elsewhere showing a parabolic dependence of contact angle on the composition of the hydrogels [39]. A recent study claimed that polymer wettability governs cell attachment more significantly than elastic stiffness [40].

Researchers have also demonstrated maximal cell adhesion to polymers on surfaces of moderate water wettability than on surfaces of high or low water wettabilities. The optimum wettability of a substrate for the culturing of fibroblasts has been estimated to be in the range between 55 and 75°. For epithelial cells, respective values have been reported to be in the range of 45–75° [41–43]. The wettability of PVA hydrogels lie well within these ranges and, thus, exhibit moderate hydrophilicity suitable for cell attachment. Here, the 14% PVA hydrogel had the highest contact angle, i.e., 65°, and the lowest surface energy value of 45 J/m² whilst maximum cell attachment was observed on the 16% PVA hydrogels which had a smaller contact angle but higher stiffness. These results signify the fact that it is a combination of suitable wettability and stiffness (along with chemistry) that altogether affects cell attachment on a hydrogel surfaces [44, 45]. The increased number of –OH groups present on the surface increase the

Fig. 4 **a** Swelling ratios of the PVA hydrogels as a function of PVA concentration. **b** Crosslinking density variation of PVA hydrogels as computed from the Flory-Rehner equation

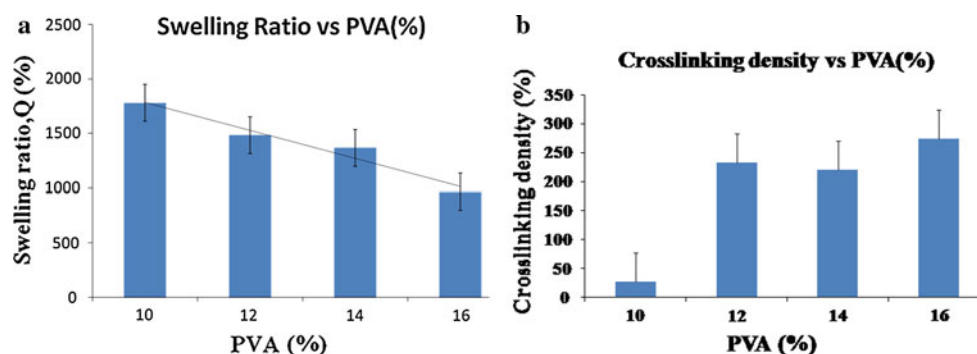
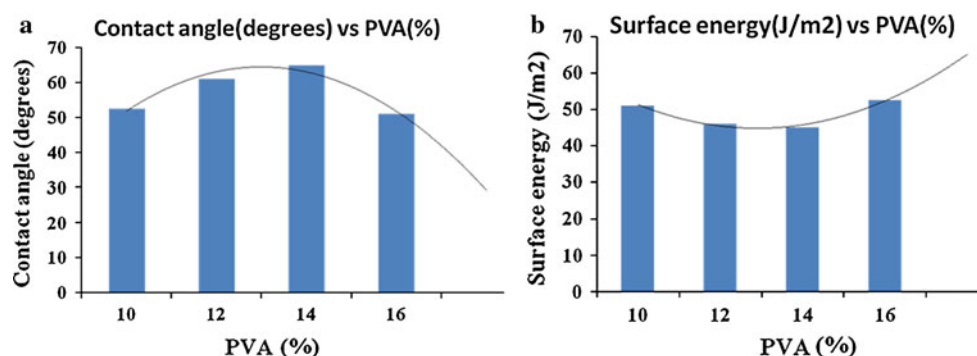


Fig. 5 Variation of **a** optical contact angle ($^{\circ}$) and **b** surface energy (J/m^2) of the hydrogel samples as a function of PVA concentration



freedom of polymer chain rearrangement for minimizing the total surface energy of the system and thus increasing the contact angle [46].

3.1.4 Cell adhesion studies

The fluorescent microscope pictures of human dermal fibroblasts and lens epithelial cells attached on the control

(glass coverslip) are shown in Fig. 6a. These are representative of what is seen for all regions on the gels. Clearly evident is the higher number of fibroblasts than epithelial cells. Figure 6b shows the number (%) of adherent fibroblasts on hydrogels after 4 h, 24 h and 3 days. The time points being compared are 4 h and 3 days. This image clearly reveals the role that polymer concentration plays in the adhesion of fibroblasts. Cells were readily attached to

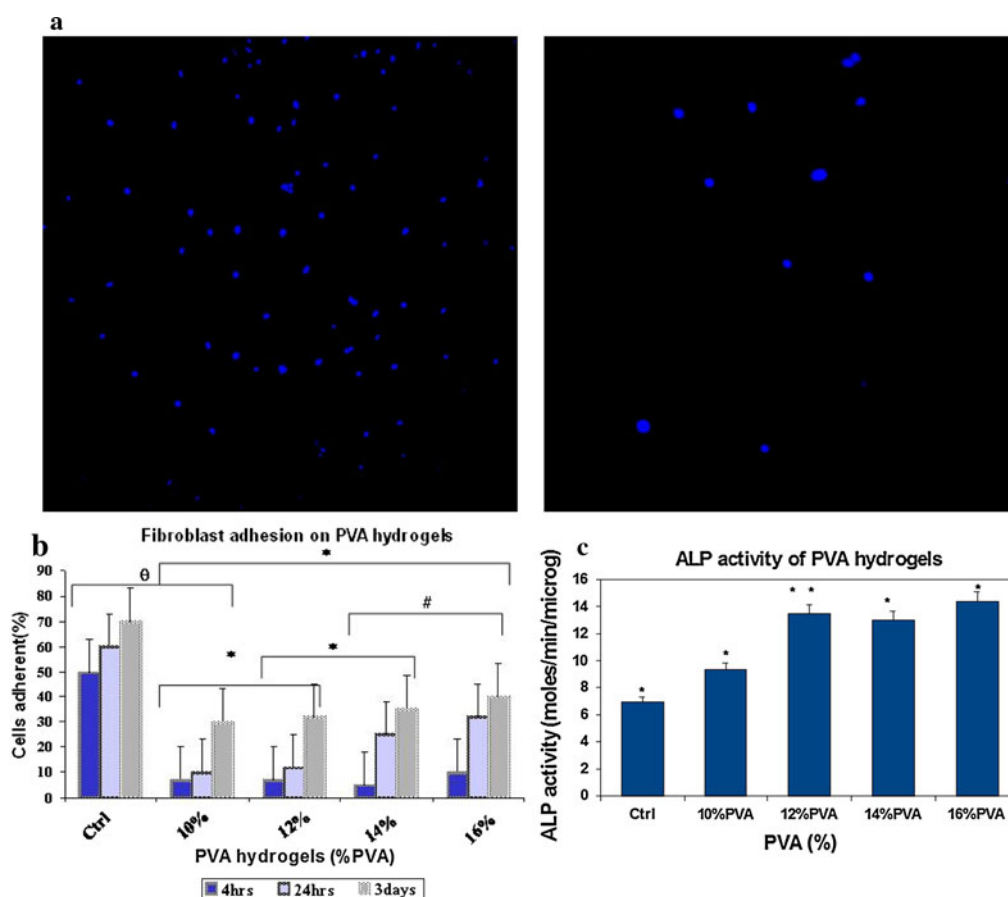
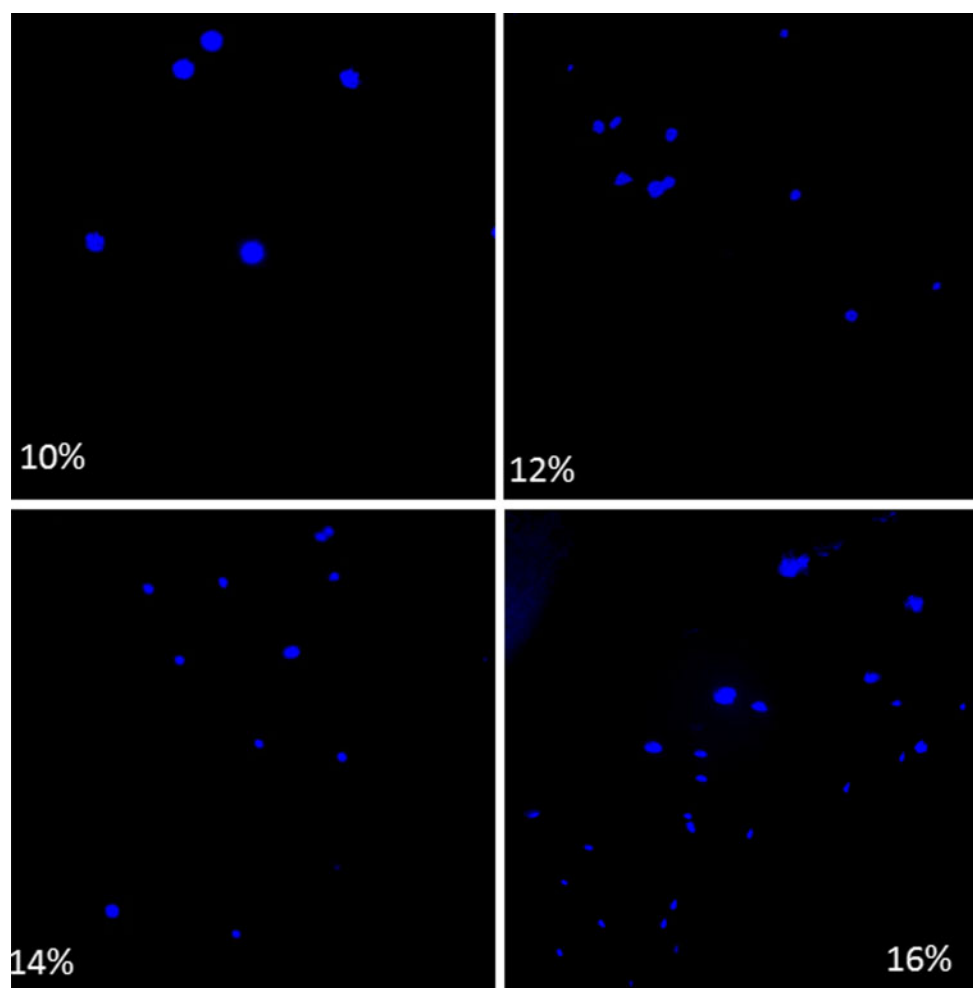


Fig. 6 **a** Fluorescence microscope images of fibroblasts and lens epithelial cells attached on controls; DAPI staining, 10 \times ; increased fibroblast attachment was observed than epithelial cells under the same conditions (3500 cells/ cm^2 seeded). **b** A curve showing the fibroblast cells attached (%) on the PVA hydrogels after 4 h, 24 h and

3 days. Error bars are mean + standard deviations ($n = 3$), $\theta = P < 0.005$, $*P < 0.05$, $^{\#}P < 0.05$. **c** A curve showing the phosphatase activity of PVA hydrogels (after 7 days) as a function of PVA concentration, error bars are mean + standard deviation ($n = 3$), $*P < 0.05$, $**P < 0.01$

Fig. 7 Fluorescent microscope images of human lens epithelial cells attached on the PVA hydrogels after 4 h



the hydrogels and their number increased with polymer concentration which can be attributed to the different topographies and wettabilities of all the compositions [47, 48]. It was evident here that the control had more fibroblasts attached than the hydrogels. The cells were found to be more comfortable on such a flat surface and they showed uniform spreading, while on the hydrogel surfaces, their spreading was non-uniform, i.e., at some places aggregates of cells were seen.

It has been established by certain groups that particularly fibroblasts and epithelial cells prefer stiffer substrates to attach [49, 50]. We found similar results here where the number of adherent cells increased as a function of polymer concentration following the degree of crystallinity, crosslinking density and tensile strength. The significance of the relationship between mechanical properties and crosslinking density of the hydrogels towards cell attachment thus needs explanation. Cells always experience mutual tension in any given tissue in any ECM. Their responses to these forces (or stresses) can vary from morphological changes to changes in specific gene expression.

Because of this, the hydrogel scaffolds need to be designed with tissue specific mechanical properties so that the fate of cells entrapped on/within them can mimic that of the natural tissue [40]. Our study has established a systematic structure-property correlation for cell attachment on transparent PVA hydrogels with a range of tensile strength and degree of crosslinking.

To check for the normal growth of cells in the polymer matrix, fibroblasts entrapped within the hydrogel matrices were studied for ALP [34, 51, 52]. Figure 6c clearly demonstrates that the content of internal and membrane bound ALP on fibroblasts cultured on all the PVA compositions increased with increasing PVA concentration. We have typically used super confluent cells in order to measure appreciable amounts of ALP unlike the adhesion test as prior experience indicates this seeding density and cell culture time is appropriate for ALP assays. The increased ALP activity seen with increasing PVA (%) could be due to there being more cells present with increasing PVA (%) but this cannot be concluded because the control which shows the greatest number of cells shows the lowest ALP activity.

However, one assumption could be made based on the fact that the three-dimensional matrices may have a greater number of cells infiltrated within them due to pores, which, is not possible with the control substrate.

To evaluate the behavior of PVA towards other cell lines than fibroblasts, human lens epithelial cells were also used in the present study. Figure 7 shows the fluorescent microscope images of the epithelial cells attached on the PVA hydrogels. After 4 h, the number of these cells attached was less as compared to fibroblasts. It is hereby implied that PVA hydrogel surfaces were more favorable towards fibroblasts than epithelial cells. However, like fibroblasts, these cells also showed increased adhesion on hydrogels with a higher concentration of PVA.

The above studies suggest the potential of these hydrogels to be used for two different applications which require further study: skin as well as ophthalmic tissue regeneration. From an ophthalmic point of view, these results are of extreme importance as this seems to be the first report where pure PVA could be transformed into a transparent, strong and, most importantly, an epithelial cell adhesive matrix. Practically, the only limitation in this regard seems to be swelling of the gels which can be controlled by further optimizing physical parameters of the hydrogels.

4 Conclusions

Transparent and mechanically tough PVA hydrogels were obtained after 45 cycles of freeze-thawing in this study and were tested in vitro for their adhesion with human dermal fibroblasts and human lens epithelial cells. The large number of both cell lines attaching onto the hydrogel surface increased the possibility of using pure PVA (without crosslinking agents) for tissue regeneration. The correlation between cell attachment and optimum values of composition dependent structural properties could be understood as both fibroblasts and epithelial cells prefer polymer substrates with high stiffness and crosslinking density. We have also shown that fibroblasts seeded on these hydrogels produce positive and systematic results with ALP tests as these functions need to be well addressed in future. Thus, it can be postulated that pure PVA hydrogels prepared with this method possess the desired features of tissue engineering scaffolds, i.e., biocompatibility, cell attachment, strength and elasticity with an additional advantage of transparency.

Acknowledgments The authors acknowledge CSIR network project NWP0035 and IUSSTF (Indo-US Science and Technology Forum) for providing the financial support under the project Biomaterials for Health Care. The authors also acknowledge the Polymer Engineering Department of Birla Institute of Technology, Ranchi for conducting the wettability studies.

References

- Hoffman AS. Hydrogels for biomedical applications. *Adv Drug Del Rev*. 2002;54(1):3–12.
- Peppas NA, Hilt JZ, Khademhosseini A, Langer R. Hydrogels in biology and medicine. *Adv Mater*. 2006;18:1345–1360.
- Rein VU, Nurguse B, Jayawarna V, Thornton PD, Simon JT, Mart RJ, Smith MA, Gough Julie E. Bioresponsive hydrogels. *Mater Today*. 2007;10(4):40–8.
- Schexnailder P, Schmidt G. Nanocomposite polymer hydrogels. *Coll Polym Sci*. 2009;287(1):1–11.
- Langer R, Peppas NA. Advances in biomaterials, drug delivery, and bionanotechnology. *Bioeng. Food Nat Product*. 2003;49(12):2990–3006.
- Arumuganathan S, Jayasinghe SN. Living scaffolds (specialized and unspecialized) for regenerative and therapeutic medicine. *Biomacromolecules*. 2008;9:759–66.
- Molly SS. Polymer scaffolds for biomaterials applications. *Macromolecules*. 2010;43:581–91.
- Kuen YL, Mooney DJ. Hydrogels for tissue engineering. *Chem Rev*. 2001;101(7):1869–80.
- Padavan DT, Hamilton AM, Millon LE, Boughner DR, Wan W. Synthesis, characterization and in vitro cell compatibility study of a poly (amic acid) graft/cross-linked poly (vinyl alcohol) hydrogel. *Acta Biomater*. 2011;7(1):258–67.
- Hassan CM, Peppas NA. Structure and applications of poly (vinyl alcohol) hydrogels produced by conventional crosslinking or by freezing/thawing methods. *Adv Polym Sci*. 2000;153:37–65.
- Bolto B, Tran T, Hoang M, Zonglie X. Crosslinked poly(vinyl alcohol) membranes. *Prog Polym Sci*. 2009;34(9):969–81.
- Ricciardi R, D' Errico G, Auriemma F, Ducouret G, Tedeschi AM, De Rosa C, Laupretre F, Lafuma F. Short time dynamics of solvent molecules and supramolecular organization of poly(vinyl alcohol) hydrogels obtained by freeze/thaw techniques. *Macromolecules*. 2005;38(15):6629–39.
- Hongbin L, Wenke Z, Weiqing X, Zhang X. Hydrogen bonding governs the elastic properties of poly(vinyl alcohol) in water: single-molecule force spectroscopic studies of PVA by AFM. *Macromolecules*. 2000;33:465–9.
- Masanori K, Hyon SH. Development and evaluation of polyvinyl alcohol—hydrogels as an artificial articular cartilage for orthopedic implants. *Materials*. 2010;3(4):2753–71.
- Nayak S, Lyon LA. Soft nanotechnology with soft nanoparticles. *Angewandte Chemie Int Ed*. 2005;44(47):7686–708.
- Cheng CM, Le Due PR. Micropatterning poly vinyl alcohol as a biomimetic material through soft lithography with cell culture. *Molec Biosys*. 2006;2(6):299–304.
- You SJ, Ahn WS, Jang HS, Kang MII, Chun HJ, Lim YM, Nho YC. Preparation and characterization of gelatin-Poly (vinyl alcohol) hydrogels for three dimensional culture. *J Ind Eng Chem*. 2007;13(1):116–20.
- Vrana NE, Liu Y, Mc Guinness BG, Cahill PA (2008) Characterization of poly (vinyl alcohol)/chitosan hydrogels as vascular tissue engineering scaffolds. *Macromol Symp*. 2008;269:106–110.
- Nuttelman CR, Henry SM, Anseth KS. Synthesis and characterization of photocrosslinkable, degradable poly(vinyl alcohol)-based tissue engineering scaffolds. *Biomaterials*. 2002;23:3617–26.
- Wang J, Gao C, Zhang Y, Wan Y. Preparation and in vitro characterization of BC/PVA hydrogel composite for its potential use as artificial cornea biomaterial. *Mater Sci Eng C*. 2010;30:214–8.
- Nuttelman CR, Mortisen DJ, Henry SM, Anseth KS. Attachment of fibronectin to poly (vinyl alcohol) hydrogels promotes NIH3T3 cell adhesion, proliferation and migration. *J Biomed Mater Res*. 2001;57(2):217–23.

22. Gupta S, Pramanik AK, Kailath A, Mishra T, Guha A, Nayar S, Sinha A. Composition dependent structural modulations in transparent poly(vinyl alcohol) hydrogels. *Coll surf B*. 2009;74(1):186–90.
23. Gupta S, Sinha S, Sinha A. Composition dependent mechanical response of transparent poly(vinyl alcohol) hydrogels. *Coll Surf B*. 2010;78(1):115–9.
24. Jason WN, Koshy ST, Bae H, Hwang CM, Yamanlar S, Khademhosseini A. Cell-laden microengineered gelatin methacrylate hydrogels. *Biomaterials*. 2010;31(21):5536–44.
25. Miyashita H, Shimmura S, Kobayashi H, Taguchi T, Asano-Kato N, Uchino Y, Masabumi K, Shimazaki Jun, Tanaka J, Tsubota K. Collagen-immobilized poly (vinyl alcohol) as an artificial cornea scaffold that supports a stratified corneal epithelium. *J Biomed Mater Res Part B*. 2005;76B(1):56–63.
26. Bunn CW. Crystal structure of poly (vinyl alcohol). *Nature*. 1948;161:929–30.
27. Po-Da H, Hong Chen J, Wu H-L. Solvent effect on structural change of poly (vinyl alcohol) physical gels. *J App polym sci*. 1998;69:2477–86.
28. Auriemma F, Rosa CD, Ricciardi R, Celso FL, Triolo R, Pipich V. Time resolving analysis of cryotropic gelation of water/poly vinyl alcohol solutions vis small angle neutron scattering. *Phys Chem B*. 2008;112(3):816–23.
29. Hassan CM, Peppas NA. Structure and morphology of freeze/thawed PVA hydrogels. *Macromolecules*. 2000;33:2472–9.
30. Ricciardi R, Auriemma F, De Rosa C. Structure and properties of poly (vinyl alcohol) hydrogels by freeze/thaw techniques. *Macromol Symp*. 2005;222(1):49–64.
31. Ricciardi R, Mangiapia G, Lo Celso F, Paduano L, Triolo R, Auriemma F, Rosa CD, Lauprete F. Structural organization of Poly (vinyl alcohol) hydrogels obtained by freezing and thawing techniques: a SANS study. *Chem Mater*. 2005;17(5):1183–9.
32. Bonakdar S, Emami SH, Shokrgozar MA, Farhadi A, Hoshiyar Ahmadi SA, Amanzadeh A. Preparation and characterization of poly vinyl alcohol hydrogels crosslinked by biodegradable polyurethane for tissue engineering of cartilage. *Mat Sci Eng C*. 2010;30(4):636–43.
33. Nagura M, Hamano T, Ishikawa H. Structure of poly (vinyl alcohol) hydrogel prepared by repeated freezing and melting. *Polymer*. 1989;30(4):762–5.
34. Wan WK, Campbell G, Zhang ZF, Hui AJ, Boughner DR. Optimizing the tensile properties of polyvinyl alcohol hydrogel for the construction of a bioprosthetic heart valve stent. *J Biomed Mater Res*. 2002;63(6):854–61.
35. Schmedlen RH, Masters KS, West JL. Photocrosslinkable poly vinyl alcohol hydrogels that can be modified with cell adhesion peptides for use in tissue engineering. *Biomaterials*. 2002;23(22):4325–32.
36. Ricciardi R, Auriemma F, Gaillet C, De Rosa C, Lauprete F. Investigation of the crystallinity of freeze/thaw poly(vinyl alcohol) hydrogels by different techniques. *Macromolecules*. 2004;37(25):9510–6.
37. Arndt KF, Richter A, Ludwig S, Zimmermann J, Kressler J, Kuckling D, Adler HJ. Poly(vinyl alcohol)/poly (acrylic acid) hydrogels: FT-IR spectroscopic characterization of crosslinking reaction and work at transition point. *Acta Polymer*. 1999;50:383–90.
38. Hassan CM, Trakampan P, Peppas NA. Water solubility characteristics of poly(vinyl alcohol) and gels prepared by freezing/thawing processes. *Water Sol Polymer*. 2002;31–40. doi:10.1007/0-306-46915-4_3.
39. Cai L, Wang S. Parabolic dependence of material properties and cell behavior on the composition of polymer networks via simultaneously controlling crosslinking density and crystallinity. *Biomaterials*. 2010;31(29):7423–34.
40. Groth T, Seifert B, Malsch G, Albrecht W. Interaction of human skin fibroblasts with moderate wettable PAN copolymer membranes. *J Biomed Mater Res A*. 2001;61(2):290–300.
41. Mei Y, Saha K, et al. Combinatorial development of biomaterials for clonal growth of human pluripotent stem cells. *Nat Mater*. 2010;9:768–78.
42. Lydon MJ, Minett TW, Tighe BJ. Cellular interactions with synthetic polymer surfaces in culture. *Biomaterials*. 1985;6:396–402.
43. Fitton JH, Dalton BA, Beumer G, Johnson G, Griesser HJ, Steele JG. Surface topography can interfere with epithelial tissue migration. *J Biomed Mater Res*. 1998;42:245–57.
44. Correlation of proliferation. Morphology and biological responses of fibroblasts on LDPE with different surface wettability. *J Biomater Sci Polymer Edn*. 2007;18:609–22.
45. Lavik E, Langer R. Tissue engineering: current state and perspectives. *App Microb Biotech*. 2004;65:1–8.
46. Kim JH, Shin DS, Ho HM, Kwon OW, Lee HK. Surface free energy analysis of poly(vinyl alcohol) films having various molecular parameters. *J Appl Polym Sci*. 2007;105:424–8.
47. Schulte Vera A, Mar D, Moller M, Lensen MC. Surface topography induces fibroblast adhesion on intrinsically non adhesive poly (ethylene glycol) substrates. *Biomacromolecules*. 2009;10:2795–801.
48. Pettit DK, Horbett TA, Hoffman AS, Chan KY. Quantitation of rabbit corneal epithelial cell outgrowth on polymeric substrates in vitro. *Invest Ophthal Vis Sci*. 1990;31:2269–77.
49. Moon JJ, Lee SH, West JL. Synthetic biomimetic hydrogels incorporated with ephrin-a1 for therapeutic angiogenesis. *Biomacromolecules*. 2007;8:42–9.
50. Mitragotri S, Lahann J. Physical approaches to biomaterial design. *Nat Mater*. 2009;8:15–23.
51. Slaughter BV, Khurshid SS, Fisher OZ, Khademhosseini A, Peppas NA. Hydrogels in regenerative medicine. *Adv Mater*. 2009;21:3307–29.
52. Yang F, Williams G, Wang CD, Lee H, Manson PN, Elisseeff J. The effect of incorporating RGD adhesive peptide in polyethylene glycol diacrylate hydrogel on osteogenesis of bone marrow stromal cells. *Biomaterials*. 2005;26(30):5991–8.